Journal of Nuclear Medicine, published on August 19, 2021 as doi:10.2967/jnumed.121.262295

Biokinetics and Dosimetry of [^{177}Lu]Lu-Pentixather

Heribert Hänscheid[1], Andreas Schirbel[1], Philipp Hartrampf[1], Sabrina Kraus[2], Rudolf A. Werner[1], Hermann Einsele[2], Hans-Jürgen Wester[3], Michael Lassmann[1], Martin Kortüm[2], and Andreas K. Buck[1]

1) Department of Nuclear Medicine, University Hospital Würzburg, Würzburg, Germany
2) Department of Internal Medicine II, University Hospital Würzburg, Würzburg, Germany
3) Department of Pharmaceutical Radiochemistry, TU Munich, Munich, Germany

Corresponding author:
Heribert Hänscheid, PhD
Department of Nuclear Medicine, Universitätsklinikum Würzburg
Oberdürrbacher Str. 6
97080 Würzburg, Germany
Phone: +49 931 201 35533
Email: haenscheid_h@ukw.de

Short title

Pentixather biokinetics and dosimetry

ABSTRACT

The chemokine receptor CXCR4, which is overexpressed in many solid and hematologic malignancies, can be targeted for radiopeptide therapy via the antagonist Pentixather®. Biokinetics and dosimetry of ^{177}Lu-Pentixather and ^{90}Y-Pentixather were analyzed.

Methods: This retrospective study is a standardized reevaluation of data collected for treatment planning. Nineteen patients with complete sets of planar whole-body scans over at least four days and a single SPECT/CT after 200 MBq ^{177}Lu-Pentixather were included. Kinetics were measured in the whole body, in tissues with activity retention, and in 10 individuals in the blood. Time-integrated activity coefficients and tissue absorbed doses were derived.

Results: Increased uptake of Pentixather was observed in kidneys, liver, spleen, and bone marrow, inducing median (minimum-maximum) absorbed doses of 0.91 (0.38-3.47), 0.71 (0.39-1.17), 0.58 (0.34-2.26), and 0.47 (0.14-2.33) Gy per GBq ^{177}Lu-Pentixather and 3.75 (1.48-12.2), 1.61 (1.14-2.97), 1.66 (0.97-6.69), and 1.06 (0.27-4.45) Gy per GBq ^{90}Y-Pentixather, respectively. In most tissues, activity increased during the first day after the administration of ^{177}Lu-Pentixather and afterwards decayed with mean effective half-lives of 41 ± 10 (range: 24-64) hours in kidneys and median half-lives of 109, 86, and 92 hours in liver, spleen, and bone marrow, respectively. Maximum uptake per kidney was 2.2% ± 1.0% (range: 0.6%-5.1%). In organs showing no specific uptake, absorbed doses exceeding 0.3 Gy per GBq ^{90}Y-Pentixather are estimated for the urinary bladder and for tissues adjacent to accumulating organs such as the adrenal glands, bone surface, and gallbladder. Dose estimates for tumors and extramedullary lesions ranged from 1.5 to 18.2 Gy per GBq ^{90}Y-Pentixather.

Conclusions: In patients with hematologic neoplasms, absorbed doses calculated for bone marrow and extramedullary lesions are sufficient to be effective as an adjunct to high-dose chemotherapies prior to stem cell transplantation.

Keywords

Pentixather; biokinetics; dosimetry; CXCR4; endoradiotherapy

INTRODUCTION

The chemokine receptor 4 (CXCR4) influences the development of malignant diseases by activating various signaling pathways that influence cell proliferation, angiogenesis, metastasis, and therapeutic resistance (*1*). On the other hand, being overexpressed in many solid and hematological neoplasms, CXCR4 is a promising target structure for radioligand therapy (*2*). A CXCR4 antagonist that has already been used in the therapy of various malignant diseases is the peptide Pentixather labeled with ^{177}Lu or ^{90}Y (*3-8*). Pentixather and its Lu- and Y-complexes exhibit high selectivity and specificity as well as good binding affinities to human CXCR4 (*4*). In blood, ^{177}Lu-Pentixather shows high binding to serum albumin, CXCR4-mediated binding to leukocytes and platelets, and excellent metabolic stability with virtually no tracer degradation (*4*).

The present report provides results of a uniformly performed dosimetric re-evaluation of measurements after pre-therapeutic administration of ^{177}Lu-Pentixather to 19 patients. This compound was originally intended to be used for both dosimetry and therapy. Since ^{90}Y-Pentixather proved to be preferable for therapy, pretherapeutic dosimetry with low ^{90}Y activities is not possible, and Pentixather labeled with a diagnostic nuclide such as ^{111}In has not yet been produced and tested, the nuclide ^{177}Lu was continued to be used for dosimetry and ^{90}Y for therapy.

MATERIALS AND METHODS

Patients

All patients with dosimetric studies with ^{177}Lu-Pentixather and measurements up to at least 4 days after the administration from June 2014 to December 2019 were considered for this retrospective analysis. A boy aged 8 years was excluded, although no obvious differences in activity kinetics were apparent as compared with adults. After excluding one study that had to be repeated, 19 studies were eligible for inclusion. The patients (11 females, 8 males; age: 40-75 y, mean: 60 ± 9 y) suffered from multiple myeloma (n=9), acute myeloid leukemia (3), diffuse large B-cell lymphoma (n=2), pre-B acute lymphoblastic leukemia (n=1), T-cell leukemia (n=1),

adrenocortical carcinoma (n=2), or thymoma (n=1) and had been treated before by multiple lines of chemotherapy (n=19), stem-cell transplantation (autologous n=10; allogeneic n=5), and external beam radiation therapy (n=9). One patient (P7) had only one kidney. Details on the included individuals are shown in Table 1.

At the time of study inclusion, all patients were refractory with exhausted standard treatment options. Based on German Drug Law, §13(2b), and after evaluation by an interdisciplinary panel of specialists, the potential benefit of CXCR4-targeted endoradiotherapy in combination with high-dose chemotherapy and stem-cell transplantation was investigated. All patients signed written informed consent and the local ethics committee expressed no objections to the retrospective evaluation and publication of the data in accordance with data protection regulations (reference number 20200915 01).

Radiochemistry

For pre-therapeutic dosimetry, ^{177}Lu-Pentixather is synthesized by adding a solution of 75 µg Pentixather (PentixaPharm, Würzburg, Germany) and 3.5 µg gentisic acid in 525 µl sodium acetate buffer solution (0.4 M, pH 5.2) to a vial containing about 300 MBq no-carrier-added $^{177}LuCl_3$ (ITG, Garching, Germany; isomeric purity: $<10^{-7}$ ^{177m}Lu) in 200 µl 0.04 M HCl, and heating the vial for 35 min at 100°C. After cooling, the solution is diluted with saline, passed through a 0.22 mm sterile filter, and tested for radiochemical purity by gradient high-performance liquid chromatography and thin layer chromatography. Bubble point and pH-value are determined before releasing the product.

The radiosynthesis of ^{90}Y-Pentixather for therapy follows the same protocol but using higher amounts of Pentixather (200 µg), gentisic acid (7 µg), and radioactivity (2-10 GBq $^{90}YCl_3$).

Measurements and Data Evaluation

Each patient received about 200 MBq ^{177}Lu-Pentixather (Supplemental Table 1) for pre-therapeutic dosimetry in order to confirm eligibility for treatment and to determine the maximum therapeutic activity. The radiopharmaceutical was administered without concomitant medication to protect the kidneys. Activity kinetics were analyzed in whole body, kidney, liver, spleen, red marrow, and tumorous lesions from repeated whole body

scans and a SPECT/CT for normalisation to absolute activity concentrations.

Whole body scans were performed with the same dual head gamma camera and identical camera settings at 0.1 h, 4 h, 1 d, 2 d, and at 4 d or later after the activity administration. Additional scans after 1 h or 3 d were included if available. For accumulating tissues, net counts were extracted from appropriate regions of interest and fitted by a decay function using ordinary least squares regression. For details see Supplemental "Whole body scans" with Supplemental Figures 1 and 2.

Total body net counts were normalized to the net counts observed in the first scan at 0.1 h. For other tissues, estimates of time-integrated activity coefficients and the specific absorbed doses, i.e. the absolute absorbed doses per unit administered activity, were deduced by normalizing the kinetics to activity concentrations measured one day (two days in patient P9) after the administration by SPECT/CT (see Supplemental "Tomographic imaging" with Supplemental Figure 3).

When possible, activity in organs was entirely quantified in SPECT/CT. In large organs, livers and enlarged spleens, activity was quantified in a partial volume and activity was scaled to the complete mass measured by CT. For the red bone marrow, the activity time function was determined in the planar images with a large region of interest over pelvis and spine and normalized to the activity measured in SPECT/CT in L2-L4 in the lumbar spine, which was assumed to contain 6.7% of the total red marrow activity (*9*).

In a subgroup of 10 patients, blood samples were collected concomitantly with the whole body scans. The whole blood activity concentrations were measured and the time-integrated activity coefficients per liter of blood were calculated by integration of a tri-exponential fit function over time.

From the kinetics measured with ^{177}Lu-Pentixather, those expected for ^{90}Y-Pentixather were calculated by converting the decay constants to the shorter physical half-life of ^{90}Y (64.0 h instead of 159.5 h for ^{177}Lu).

The free internal dosimetry software IDAC-DOSE 2.1 (*10*) was used to determine specific absorbed doses in evaluated tissues from the measured time-integrated activity coefficients per unit mass scaled to the gender specific reference masses and multiplied by the organ and gender specific S-values in IDAC-DOSE 2.1. The software was also used to estimate absorbed doses in unevaluated tissues from the medians of the measured time-

integrated activity coefficients and the kidney-bladder model as describes in (*11*) with 3.5 h voiding interval. The percentage of total body activity not located in the evaluated accumulating tissues was attributed to the remainder of the body.

The free software JASP (*12*) was used for statistical analyses. The distributions determined in this study were tested for normal distribution using the Shapiro-Wilk test with rejection of the null hypothesis for $p<0.05$. Parameters of normally distributed data are reported as mean ± standard deviation (range: minimum to maximum), otherwise median (quartiles: minimum, 1st quartile, 3rd quartile, maximum) are shown.

RESULTS

The biokinetics of ^{177}Lu-Pentixather was heterogeneous in the group of included patients. Figure 1 shows the whole body scans two days after the administration of the diagnostic activity in three of the patients: patient P7 with only one kidney showed the highest specific absorbed doses measured for kidneys and livers, P15 with pre-B acute lymphoblastic leukemia the highest specific absorbed dose observed in red marrow and spleens as well as the highest whole body time-integrated activity coefficient, and P2 with multiple myeloma presented the highest specific absorbed dose in an extramedullar lesion and the highest time-integrated activity coefficient per liter of blood.

Tables 2 and 3 list the time-integrated activity coefficients and specific absorbed doses for the evaluated tissues for ^{177}Lu-Pentixather and ^{90}Y-Pentixather, respectively. Figure 2 shows typical time functions of activity retention in organs and tissues exemplified by patient P3.

The red bone marrow is the dose-limiting organ when the absorbed dose is limited to 2 Gy to preserve function. The mean effective half-life in the bone marrow was 97 h ± 31 h (range: 39 h to physical half-life) after ^{177}Lu (kinetics decay corrected to ^{90}Y: 50 ± 9 h; range: 29 h to physical half-life). In 14 patients, the red marrow activity concentration initially increased and reached a maximum at 23 ± 11 h after the administration before decreasing.

If stem cell support is available and myeloablation is tolerated or intended, the therapeutic activity is not limited by the red marrow but the absorbed dose to the kidneys (23 Gy). This would have increased the tolerable activity by a median factor of 4.9 (range: 1.6 to 70.9) after ^{177}Lu and a factor of 2.8 (range: 1 to 34.7) after ^{90}Y even without renal protective medication. Uptake per kidney generally increased at 4 h and later up to a mean maximum of 2.2% ± 1.0% (range: 0.6% to 5.1%) of the administered activity at 18 ± 7 h after the administration and a subsequent decrease with a mean effective half-life of 41 ± 10 h (range: 24 h to 64 h). The fitted half-life of the increasing component was 27 h in Patient P7 and a median 7.8 h (quartiles: 2.4 h, 4.9 h, 12.2 h, 15.4 h) in patients with two kidneys. Decay-corrected to ^{90}Y, the mean maximum uptake would have been 1.9% ± 0.9% (range: 0.5% to 4.0%) after 14 ± 6 h and the mean effective half-life 29 ± 5 h (range: 20 h to 40 h).

Compared to kidneys, kinetics in livers was retarded with a later maximum of retention (6.1% ± 1.8%; range: 2.2% to 10.0%) after 35 ± 11 h and a longer median effective half-live of 109 h (quartiles: 77 h, 92 h, 146 h, physical half-life) after ^{177}Lu. Respective data for ^{90}Y-Pentixather would have been 4.9% ± 1.6% (range: 1.8% to 8.6%) retention after 23 ± 7 h and a median effective half-life of 54 h (quartiles: 45 h, 49 h, 54 h, physical half-life).

High values of the time-integrated activity coefficient for the spleen (Tables 2 and 3) were associated with splenomegaly due to malignant infiltration. In affected patients, a high absorbed dose to the spleen is considered a desirable therapeutic effect. Measured spleen masses in patients P14, P15 (Figure 1), and P16 were 824 g, 530 g, and 539 g, respectively. Fifteen patients showed a delayed retention maximum. The mean effective half-live in spleen was 99 ± 36 h (range: 51 h to physical half-life) after ^{177}Lu (^{90}Y: 50 ± 9 h; range: 35 h to physical half-life).

In malignant extramedullary lesions, activity initially almost always increased, reaching a maximum after a median of 11 h and then decreasing with effective half-lives of 122 ± 32 h (range: 78 h to physical half-life) after ^{177}Lu (^{90}Y: 56 ± 7 h; range: 45 h to physical half-life). The calculated values for the tissue absorbed doses per unit administered activity ranged from 0.7 Gy to 6.9 Gy per GBq ^{177}Lu and 1.5 Gy to 18.2 Gy per GBq ^{90}Y.

Estimates of absorbed doses in organs apparently without specific activity accumulation are shown in Supplemental Table 2. Absorbed doses of about 0.05 Gy/GBq ^{177}Lu-Pentixather and 0.2 Gy/GBq ^{90}Y-

Pentixather are expected in most organs. Somewhat higher values are estimated for the urinary bladder and for tissues adjacent to accumulating organs such as adrenals, bone surface, and gallbladder.

DISCUSSION

High and long-lasting retention of Pentixather in the bone marrow leads to high specific absorbed doses to the hematopoietic system. The estimates for the bone marrow absorbed dose indicate that the safety limit of 2 Gy is usually reached after about 4 GBq ^{177}Lu or 2 GBq ^{90}Y. The absorbed doses achievable in malignant tissues with these activities are considered insufficient to achieve an adequate therapeutic effect on malignant tissue, especially in solid tumors with moderate CXCR4 expression. In hematologic neoplasms, on the other hand, therapy with Pentixather can be a reasonable complement to high-dose chemotherapy regimens followed by subsequent hematopoietic stem cell transplantation with the potential to effectively fight radiation-sensitive lesions.

With the exception of P11, P14, and P15, who experienced unexpected obstacles regarding stem cell availability, and P5, whose health deteriorated, all patients with hematologic diseases received therapy. Patients P17, P18, and P19 with adrenocortical carcinoma or thymoma remained untreated. Patients P1to P4 received ^{177}Lu-Pentixather for treatment (see Supplemental “Post-therapeutic measurements” with Supplemental Figures 4 and 5), all others ^{90}Y-Pentixather. ^{177}Lu-Pentixather for therapy has the advantage that its gamma radiation can be used scintigraphically for the verification of the activity distribution and for dosimetry, but has an unfavorably long half-life in the bone marrow. With therapeutic doses of 10 Gy or more to the red bone marrow, the activity in the marrow must decay for at least 4 to 5 half-lives before stem cell transplantation in order to safely avoid compromising engraftment. While this is ensured 2 weeks after ^{90}Y-Pentixather, a time interval up to 4 weeks may be necessary for ^{177}Lu-Pentixather. The longer time span between ^{177}Lu-Pentixather treatment and transplantation is disadvantageous as the prolonged phase of aplasia poses an increased risk of infectious complications.

Since Pentixather, as other radiolabeled peptides, is filtered through the kidneys, activity retention in renal tubules must be considered. It is not yet known whether, as with somatostatin receptor agonists, ^{90}Y has higher

renal toxicity because of its higher beta energy and dose rate, and which renal dose limits are appropriate for Pentixather labeled with ^{177}Lu or ^{90}Y. The limit of 23 Gy for the tolerable absorbed dose, which is often used for the kidneys (*13*), is reached after 20-30 GBq ^{177}Lu-Pentixather or 5-8 GBq ^{90}Y-Pentixather in most patients. While 10 GBq ^{90}Y-Pentixather could have been safely administered in 20% of patients, the specific absorbed dose determined for the patient with only one kidney (P7) was 12.2 Gy per GBq, limiting the safely administerable activity to 1.9 GBq. In patients with two kidneys, who were not included in this study because dosimetric measurements were performed over three days only, the highest calculated dose was 12.7 Gy per GBq ^{90}Y-Pentixather.

Concomitant medication with amino acids, such as that recommended for somatostatin receptor therapy with radiolabeled peptides (*13*), also reduces retention of Pentixather in the kidneys (Supplemental Table 3). The reduction factor of 64% ± 13% (range: 50% to 80%) reported in (*8*) was derived from only six treatments with ^{177}Lu-Pentixather and remains to be validated.

The above figures indicate that, in an approach of myeloablative therapy with fixed activities, hardly more than 2.5 GBq ^{90}Y-Pentixather can be administered without exceeding a kidney dose of 23 Gy in individual patients. The estimated specific absorbed doses to bone marrow and lesions indicate that this is likely to leave many patients inadequately dosed, which strongly supports the theragnostic approach with pretherapeutic dosimetry.

In order to assess the data shown here, the following comments should be made:

The data included in the present study were not collected prospectively in an optimized study design. The dosimetric measurements were performed with the lowest activity that seemed necessary, which limits the accuracy of the scintigraphic imaging and its evaluation (see Supplemental “Uncertainties”). Some estimate of the dosimetric accuracy is provided by the intraindividual comparison of the absorbed doses determined for the right and left kidneys after ^{177}Lu-Pentixather, which incorporates the uncertainties of both volume segmentation and measurement and fit of activity kinetics. The dose derived for the right kidney was 108% ± 14% (range: 78% to 128%) of that for the left kidney.

In tissues with delayed retention maximum and a long half-life of the retained activity, namely liver, spleen, and red bone marrow, measurements over four days are often not sufficient to be able to determine the half-life with good accuracy. Later measurements, however, were not necessary to estimate the absorbed doses to the kidneys and would have required an additional patient visit and the use of higher activities, which was avoided to minimize the risk of affecting kinetics by the dose administered pretherapeutically. For therapy with ^{90}Y-Pentixather, scans over three days are sufficient to measure the kinetics in the kidneys (see Supplemental "Uncertainties").

For the ^{90}Y-Pentixather kinetics data shown here, it should be emphasized that these were generally calculated by converting the ^{177}Lu-Pentixather results assuming comparable kinetics for ^{nat}Lu and ^{nat}Y. Comparison of kinetics during therapy with prediction has not been technically possible in our patients treated with ^{90}Y-Pentixather, but is intended in the future by quantification of the positrons of the ^{90}Y decay with a PET/CT of higher sensitivity. Since the metal used affects the CXCR4 affinity and thus potentially biokinetics, deviations of actual absorbed doses from estimates are possible. The binding affinity of ^{nat}Y-Pentixather to CXCR4 is slightly lower than that of ^{nat}Lu-Pentixather (*4*), which is most likely to affect binding in target tissues. Also an influence on excretion and kinetics in healthy organs cannot generally be excluded.

An interesting alternative for the treatment of hematological malignancies could be the labeling of Pentixather with an alpha emitter to effectively target smaller cell clusters. ^{nat}Bi-Pentixather has a higher binding affinity to CXCR4 than ^{nat}Lu-Pentixather (*4*), but even for the most suitable isotope ^{213}Bi, the half-life of only 46 min is likely to be too short.

Bone marrow dosimetry is uncertain even in healthy individuals. In patients with malignant transformation of the hematologic system, the bone marrow may be severely modified in an individualized manner. The activity pattern in the medullary spaces is often very inhomogeneous and the assumption of 6.7% bone marrow content in the evaluated vertebrae is even more uncertain than in healthy subjects. The doses mentioned should therefore rather be regarded as calculated values for estimating the approximate magnitude.

CONCLUSION

The radiation absorbed doses achievable with labeled Pentixather are often insufficient for radiological destruction of solid tumors. In hematologic neoplasms, however, ^{90}Y-Pentixather can be effective against radiosensitive lesions and as a useful adjunct to the conditioning regimen prior to stem cell transplantation. While the kidneys are the dose-limiting organ in myeloablative therapy, high exposures also occur in the liver and spleen. Of the remaining organs, absorbed doses exceeding 0.3 Gy/GBq are estimated for the urinary bladder and for tissues adjacent to accumulating organs such as the adrenal glands, bone surface, and gallbladder.

DECLARATIONS

Conflict of interest/Competing interests All authors declare no conflict of interest.

Ethical approval The additional diagnostic procedures described in this report were performed in accordance with §13(2b) German Drug Act. The ethics committee expressed no objections to the retrospective evaluation and publication of the data in accordance with data protection regulations (reference number 20200803 01).

Informed consent All patients signed written informed consent to the activity administrations and the diagnostic procedures as well as to the recording and analysis of their data and the anonymized publication of the results.

KEY POINTS

Question How do the biokinetics of the CXCR4 antagonist Pentixather® affect endoradiotherapy?

Pertinent findings Dosimetric studies with 200 MBq ^{177}Lu-Pentixather in 19 patients demonstrated very heterogeneous absorbed doses per administered activity in organs and tissues and identified the red bone marrow and kidneys as dose-limiting organs.

Implications for patient care Therapy with ^{90}Y-Pentixather may be considered if the malignant tissue is radiosensitive, myeloablation is accepted, and excessive renal absorbed dose is avoided by pretherapeutic dosimetry.

REFERENCES

1. Chatterjee S, Behnam Azad B, Nimmagadda S. The intricate role of CXCR4 in cancer. *Adv Cancer Res.* 2014;124:31-82.

2. Walenkamp AME, Lapa C, Herrmann K, Wester HJ. CXCR4 ligands: the next big hit? *J Nucl Med.* 2017;58:77s-82s.

3. Herrmann K, Schottelius M, Lapa C, et al. First-in-human experience of CXCR4-directed endoradiotherapy with Lu-177- and Y-90-labeled Pentixather in advanced-stage multiple myeloma with extensive intra- and extramedullary disease. *J Nucl Med.* 2016;57:248-251.

4. Schottelius M, Osl T, Poschenrieder A, et al. [Lu-177]pentixather: comprehensive preclinical characterization of a first CXCR4-directed endoradiotherapeutic agent. *Theranostics.* 2017;7:2350-2362.

5. Habringer S, Lapa C, Herhaus P, et al. Dual targeting of acute leukemia and supporting niche by CXCR4-directed theranostics. *Theranostics.* 2018;8:369-383.

6. Lapa C, Hanscheid H, Kircher M, et al. Feasibility of CXCR4-directed radioligand therapy in advanced diffuse large B-cell lymphoma. *J Nucl Med.* 2019;60:60-64.

7. Maurer S, Herhaus P, Lippenmeyer R, et al. Side effects of CXC-chemokine receptor 4-directed endoradiotherapy with Pentixather before hematopoietic stem cell transplantation. *J Nucl Med.* 2019;60:1399-1405.

8. Lapa C, Herrmann K, Schirbel A, et al. CXCR4-directed endoradiotherapy induces high response rates in extramedullary relapsed Multiple Myeloma. *Theranostics.* 2017;7:1589-1597.

9. Shen S, Meredith RF, Duan J, et al. Improved prediction of myelotoxicity using a patient-specific imaging dose estimate for non-marrow-targeting Y-90-antibody therapy. *J Nucl Med.* 2002;43:1245-1253.

10. Andersson M, Johansson L, Eckerman K, Mattsson S. IDAC-Dose 2.1, an internal dosimetry program for diagnostic nuclear medicine based on the ICRP adult reference voxel phantoms. *EJNMMI Res.* 2017;7:88.

11. ICRP106. Radiation dose to patients from radiopharmaceuticals. Addendum 3 to ICRP Publication 53. ICRP Publication 106. Approved by the Commission in October 2007. *Ann ICRP.* 2008;38:1-197.

12. JASP-Team. JASP (Version 0.14.1)[Computer software]. *https://jasp-statsorg/ Accessed on 15 Mar 2021.*

13. Bodei L, Mueller-Brand J, Baum RP, et al. The joint IAEA, EANM, and SNMMI practical guidance on peptide receptor radionuclide therapy (PRRNT) in neuroendocrine tumours. *Eur J Nucl Med Mol Imaging.* 2013;40:800-816.

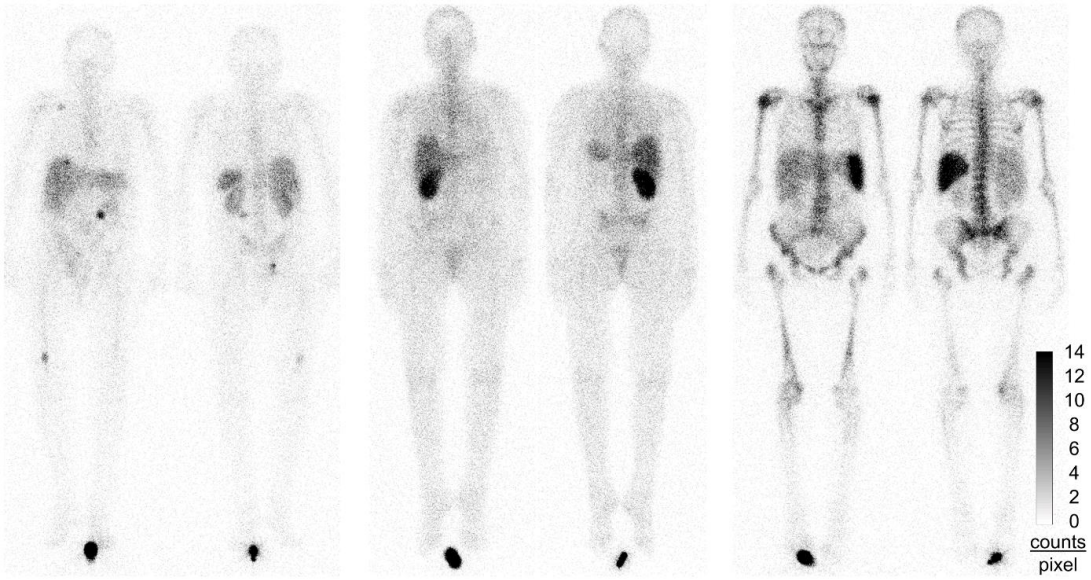

Figure 1: Examples of different activity distributions after ^{177}Lu-Pentixather in patients with multiple myeloma, P2 and P7, and patient P15 with pre-B acute lymphoblastic leukemia. While the uptake in the single kidney of patient P7 was 5%, sum of uptakes in both kidneys of patient P15 was only 1.1%. In contrast, retention was 3-fold higher in the bone marrow and 11-fold higher in the spleen of P15.

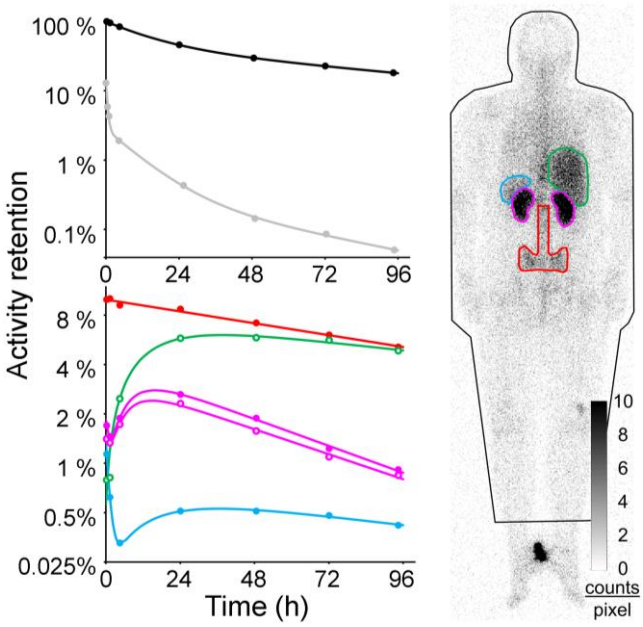

Figure 2: Regions of interest used to derive the time functions of activity retention in the whole body (black dots), red bone marrow (red dots), liver (green circles), right (purple dots) and left (purple circles) kidneys, and spleen (blue dots) in patient P3 with respective fit functions. The scintigram shows the posterior image of the whole body scan 24 hours after 197 MBq ^{177}Lu-Pentixather. The grey dots with fit function represent the activity retention per liter of whole blood.

Table 1: Patient characteristics at time of dosimetric assessment with ^{177}Lu-Pentixather

	Sex	Age (y)	Weight (kg)	Height (cm)	eGFR	Disease	since (mo)	c Tx	r Tx	auto Tx	allo Tx
P1	M	61	60	158	99	MM	18	x		1	
P2	F	66	64	163	100	MM	54	x		3	
P3	F	53	74	165	54	MM	123	x		3	
P4	M	65	93	192	46	MM	101	x		2	
P5	M	74	60	173	54	MM	22	x	x	2	
P6	M	71	80	175	79	MM	77	x	x	2	
P7	F	66	60	166	40	MM	138	x	x	1	
P8	F	57	104	157	96	MM	49	x	x	1	
P9	M	59	77	172	50	MM	23	x	x	2	
P10	M	46	70	183	92	AML	7	x			1
P11	M	60	78	182	82	AML	19	x			1
P12	F	54	62	168	67	AML	27	x			1
P13	F	64	80	163	85	DLBCL	42	x			1
P14	F	59	68	172	20	DLBCL	32	x	x	1	
P15	F	75	75	168	59	pre-B ALL	15	x			
P16	F	50	78	172	54	TCL	21	x			1
P17	F	55	64	160	96	ACC	46	x	x		
P18	M	55	90	175	92	ACC	14	x	x		
P19	F	40	52	163	n/a	Thymoma	37	x	x		

eGFR: CKD-EPI glomerular filtrate rate estimate in ml/min per 1.73 m²; n/a: not available;
MM: multiple myeloma; AML: acute myeloid leukemia; DLBCL: diffuse large B-cell lymphoma; pre-B ALL: pre-B acute lymphoblastic leukemia; TCL: T-cell leukemia; ACC: adrenocortical carcinoma; Tx: previous therapies (c: chemo; r: irradiation; auto: autologous stem-cells; allo: allogeneic stem cells)

Table 2: [^{177}Lu-Pentixather time-integrated activity coefficients (ã) in whole body (WB), organs and tumorous lesions, red marrow (RM), and blood as well as tissue absorbed doses per administered activity (D/A) in organs and lesions.

	WB	Kidneys		Liver		Spleen		RM		Lesion	Blood
	ã (h)	ã (h)	D/A (Gy/GBq)	ã (h)	D/A (Gy/GBq)	ã (h)	D/A (Gy/GBq)	ã (h)	/A (Gy/GBq)	D/A (Gy/GBq)	ã (h/l)
P1	51.6	4.39	1.01	3.8	0.39	2.06	0.58	4.0	0.14	2.2	0.21
P2	56.1	2.42	0.71	14.4	0.82	2.49	1.55	8.1	0.37	6.9	0.58
P3	55.3	4.85	2.10	15.2	0.93	1.27	0.72	14.3	0.66		0.48
P4	97.6	4.61	1.48	16.2	0.80	2.03	0.70	13.7	0.48		0.28
P5	87.7	1.92	0.87	12.2	0.91	3.71	1.59	16.8	0.59	1.7	
P6	62.1	1.74	0.50	11.7	0.62	0.63	0.34	11.8	0.41	3.1	
P7	111.0	6.25	3.47	15.0	1.17	1.34	1.12	10.6	0.48		
P8	61.6	5.28	1.21	10.0	0.39	0.90	0.38	9.4	0.43		
P9	111.6	4.76	1.12	13.2	0.67	1.18	0.47	13.6	0.47		
P10	50.5	4.51	0.90	9.0	0.43	2.47	0.40	9.9	0.35		0.32
P11	55.9	4.34	1.14	8.0	0.42	1.43	0.48	9.1	0.32		0.34
P12	77.8	2.03	0.79	13.9	0.71	3.46	0.75	21.3	0.97	1.1	
P13	114.9	7.87	0.91	21.9	0.67	2.65	0.35	22.8	1.04	2.1	
P14	83.6	1.63	0.59	16.7	0.88	11.5	1.20	16.4	0.75		
P15	140.9	1.04	0.38	15.5	0.71	14.0	2.26	51.0	2.33		
P16	108.8	3.22	1.07	14.1	0.50	6.51	1.03	12.2	0.56	1.6	0.28
P17	73.6	1.93	0.52	20.1	0.92	2.38	0.56	5.5	0.25	2.3	0.28
P18	51.6	3.47	0.67	12.0	0.41	3.30	0.42	4.0	0.14	1.1	0.32
P19	48.0	5.23	1.96	9.4	0.81	0.44	0.48	8.5	0.39	0.7	0.44
SW p	0.03	0.31	<.01	0.95	0.21	<.01	<.01	<.01	<.01	<.01	0.23
minimum	48.0	1.04	0.38	3.7	0.39	0.44	0.34	4.0	0.14	0.7	0.21
1st quartile	55.6	1.98	0.70	10.9	0.47	1.30	0.45	8.8	0.36	1.2	0.28
median	73.6	4.34	0.91	13.9	0.71	2.38	0.58	11.8	0.47	1.9	0.32
3rd quartile	103.2	4.80	1.18	15.4	0.85	3.38	1.08	15.4	0.62	2.3	0.42
maximum	140.9	7.87	3.47	21.9	1.17	14.0	2.26	51.0	2.33	6.9	0.58
mean	79.0	3.77	1.13	13.3	0.69	3.36	0.81	13.8	0.59	2.3	0.35
stdev	27.9	1.82	0.73	4.2	0.22	3.61	0.52	10.4	0.49	1.8	0.11

SW p: p-value of Shapiro-Wilk test of normality; stdev: standard deviation

Table 3: ^{90}Y-Pentixather time-integrated activity coefficients (ã) in whole body (WB), organs and tumourous lesions, red marrow (RM), and blood as well as tissue absorbed doses per administered activity (D/A) in organs and lesions (recalculated from kinetics measured with ^{177}Lu-Pentixather).

	WB	Kidneys		Liver		Spleen		RM		Lesion	Blood
	ã (h)	ã (h)	D/A (Gy/GBq)	ã (h)	D/A (Gy/GBq)	ã (h)	D/A (Gy/GBq)	ã (h)	D/A (Gy/GBq)	D/A (Gy/GBq)	ã (h/l)
P1	31.5	3.03	3.91	1.9	1.18	1.05	1.66	2.3	0.34	6.1	0.19
P2	33.6	1.90	3.16	5.8	1.91	0.95	3.30	4.0	0.77	18.2	0.48
P3	35.1	2.95	7.32	6.0	2.12	0.53	1.70	7.4	1.42		0.42
P4	51.6	2.97	5.36	6.3	1.80	0.82	1.58	6.0	0.88		0.28
P5	50.8	1.22	3.10	6.1	2.65	1.26	3.04	8.4	1.23	4.1	
P6	40.1	1.31	2.12	5.2	1.61	0.40	1.20	7.4	1.09	9.2	
P7	54.2	3.87	12.2	6.6	2.97	0.69	3.22	6.5	1.25		
P8	34.5	3.74	4.85	5.4	1.22	0.45	1.07	5.1	0.98		
P9	58.5	3.22	4.29	6.1	1.77	0.67	1.51	7.2	1.06		
P10	32.8	3.32	3.75	4.6	1.29	1.07	0.97	4.9	0.72		0.28
P11	35.7	2.83	4.21	3.8	1.16	0.76	1.42	4.7	0.69		0.30
P12	47.2	1.41	3.16	5.4	1.61	2.06	2.51	10.1	1.94	3.4	
P13	59.3	4.89	3.21	8.5	1.51	1.42	1.05	8.9	1.72	4.7	
P14	49.6	1.04	2.15	7.6	2.32	6.63	3.85	9.6	1.85		
P15	67.7	0.71	1.48	6.0	1.57	7.40	6.69	23.2	4.45		
P16	63.8	2.38	4.50	7.8	1.59	3.04	2.70	7.1	1.36	4.2	0.26
P17	41.1	1.39	2.15	8.7	2.31	1.41	1.88	3.1	0.59	5.4	0.44
P18	34.5	2.47	2.67	5.7	1.14	1.58	1.13	1.8	0.27	3.6	0.28
P19	29.9	3.53	7.52	3.6	1.80	0.25	1.53	3.5	0.68	1.5	0.40
SW p	0.08	0.53	<0.01	0.55	0.13	< .01	< .01	< .01	< .01	< .01	0.31
minimum	29.9	0.71	1.48	2.0	1.14	0.25	0.97	1.83	0.27	1.5	0.19
1st quartile	34.5	1.40	2.88	5.3	1.40	0.68	1.31	4.35	0.71	3.7	0.28
median	41.1	2.83	3.75	6.0	1.61	1.05	1.66	6.50	1.06	4.5	0.29
3rd quartile	52.9	3.27	4.67	6.4	2.02	1.50	2.87	7.88	1.39	5.9	0.41
maximum	67.7	4.89	12.2	8.7	2.97	7.40	6.69	23.2	4.45	18.2	0.48
mean	44.8	2.54	4.27	5.9	1.77	1.71	2.21	6.90	1.22	6.0	0.33
stdev	12.0	1.14	2.52	1.7	0.51	1.99	1.39	4.61	0.91	4.7	0.10

SW p: p-value of Shapiro-Wilk test of normality; stdev: standard deviation

Graphical Abstract

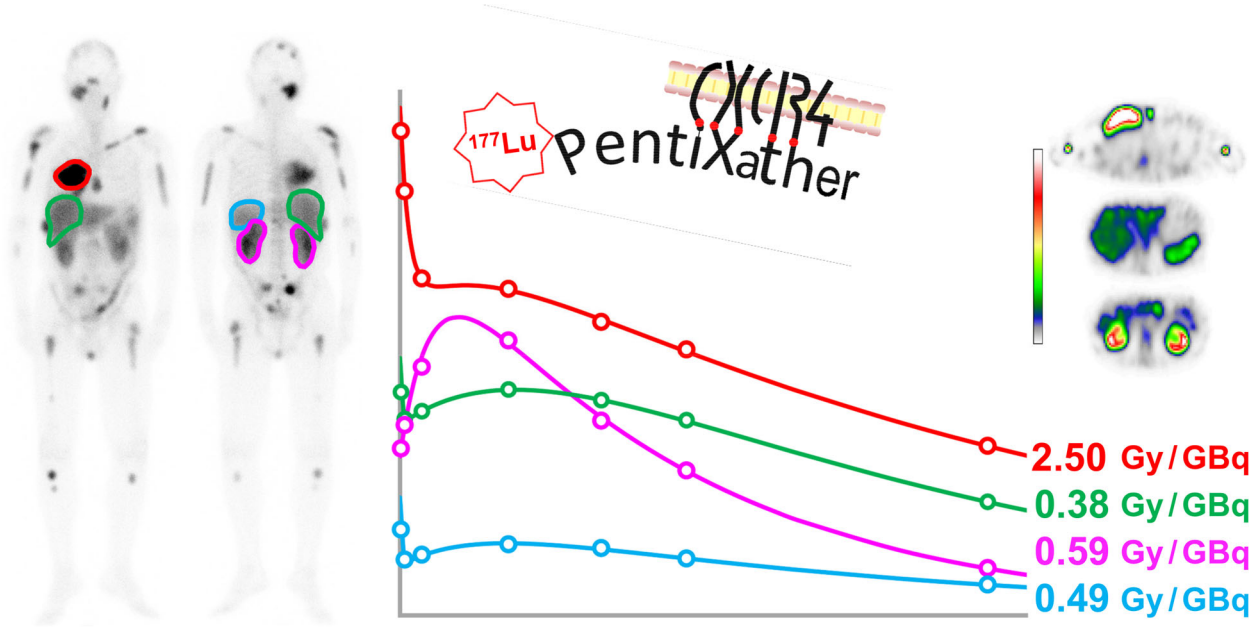

Supplemental to

Biokinetics and Dosimetry of [^{177}Lu]Lu-Pentixather and [^{90}Y]Y-Pentixather

Heribert Hänscheid[1], Andreas Schirbel[1], Philipp Hartrampf[1], Sabrina Kraus[2], Rudolf A. Werner[1], Hermann Einsele[2], Hans-Jürgen Wester[3], Michael Lassmann[1], Martin Kortüm[2], and Andreas K. Buck[1]

1) Department of Nuclear Medicine, University Hospital Würzburg, Würzburg, Germany
2) Department of Internal Medicine II, University Hospital Würzburg, Würzburg, Germany
3) Department of Pharmaceutical Radiochemistry, TU Munich, Munich, Germany

Administered activities

Activities and nuclides administered for pretherapeutic dosimetry and therapy of the patients included are listed in Supplemental Table 1. Dosimetry identified the kidneys as the dose-limiting organ. To be conservative, especially for the early therapies, activity was chosen to target at 23 Gy in the 1-mL volume with the highest activity concentration in SPECT/CT. Seven individuals remained untreated. Patient P5 became medically ineligible for therapy. Patients P11, P14, and P15 experienced unexpected problems with stem cell availability. Patients P17, P18, and P19 with solid tumors likely to require absorbed doses of several 10 Gy for effective therapy showed inadequate uptake into target tissue. All patients receiving therapy had hematologic neoplasms. Like the red marrow itself, degenerate hematologic cells in the medullary cavity, extramedullary lesions, and affected organs such as the spleen, if affected, are eliminated or at least significantly reduced at absorbed doses as low as 10 Gy and less.

Supplemental Table 1: Administered activities for pretherapeutic dosimetry and therapy

	Disease	Dosimetry	Therapy	
		(MBq ^{177}Lu)	(GBq ^{177}Lu)	(GBq ^{90}Y)
P1	Multiple myeloma	238	15.2	
P2	Multiple myeloma	199	23.5	
P3	Multiple myeloma	197	7.8	
P4	Multiple myeloma	206	9.9	
P5	Multiple myeloma	210	–	
P6	Multiple myeloma	210		6.2
P7	Multiple myeloma	197		2.2
P8	Multiple myeloma	209		5.0
P9	Multiple myeloma	207		4.9
P10	Acute myeloid leukemia	209		4.7
P11	Acute myeloid leukemia	203	–	
P12	Acute myeloid leukemia	205		5.6
P13	Diffuse large B-cell lymphoma	200		4.3
P14	Diffuse large B-cell lymphoma	212	–	
P15	pre-B acute lymphoblastic leukemia	212	–	
P16	T-cell leukemia	200		4.2
P17	Adrenocortical carcinoma	194	–	
P18	Adrenocortical carcinoma	216	–	
P19	Thymoma	199	–	

Supplemental Table 2: Absorbed dose estimates in organs without specific accumulation of Pentixather.

	Absorbed dose in Gy/GBq			
	Female		Male	
	Lu-177	Y-90	Lu-177	Y-90
Adrenals	0.09	0.52	0.08	0.57
Breast	0.06	0.22	0.05	0.18
Colon wall	0.05	0.15	0.05	0.12
Bone surface	0.24	0.72	0.19	0.56
Gallbladder wall	0.12	0.65	0.10	0.52
Heart wall	0.06	0.25	0.05	0.19
Lung	0.05	0.18	0.04	0.13
Oesophagus	0.06	0.20	0.05	0.15
Ovaries	0.07	0.22		
Pancreas	0.07	0.23	0.06	0.16
Prostate			0.06	0.21
Salivary glands	0.06	0.23	0.05	0.18
Skin	0.06	0.16	0.05	0.14
Small intestine wall	0.06	0.16	0.04	0.12
Stomach wall	0.06	0.25	0.05	0.14
Testes			0.05	0.18
Thyroid	0.06	0.21	0.05	0.17
Urinary bladder wall	0.08	0.75	0.07	0.62
Uterus/cervix	0.07	0.24		

Whole body scans

About 200 MBq ^{177}Lu-Pentixather without concomitant medication to protect the kidneys were administered to each patient for pre-therapeutic dosimetry. Activity kinetics were analyzed in whole body, kidney, liver, spleen, red marrow, and tumorous lesions. Patient imaging included a series of planar whole body scans and a SPECT/CT for normalisation to absolute activity concentrations.

All whole body scans were performed with the same dual head gamma camera (Siemens Symbia E, Siemens Healthineers, Erlangen, Germany) equipped with 15.9 mm thick scintillator crystals and medium energy collimators. Camera settings for whole body scans were 1024x256 acquisition matrix, 20% energy window at 208 keV, 10 cm/min scan speed, and identical measuring distance for all scans in a series.

All patients had whole body scans at 0.1 h, 4 h, 1 d, and 2 d post injection (p.i.) of the activity, all but 4 (P2, P5, P17, P19) at 1 h p.i., and 10 patients at 3 d p.i. (P1 to P5, P12 to P15, P18). The last scan was performed after 4 d except for P9 (5 d), P1 (6 d), and P4 and P14 (7 d). Supplemental Figure 1 shows a complete series of 7 whole body scans of patient P3.

Regions of interest (ROI) were drawn including the tissue under consideration, or part of the tissue in case of overlapping accumulating tissues, and over an area with representative background adjacent to the tissue ROI (Supplemental Figure 2).

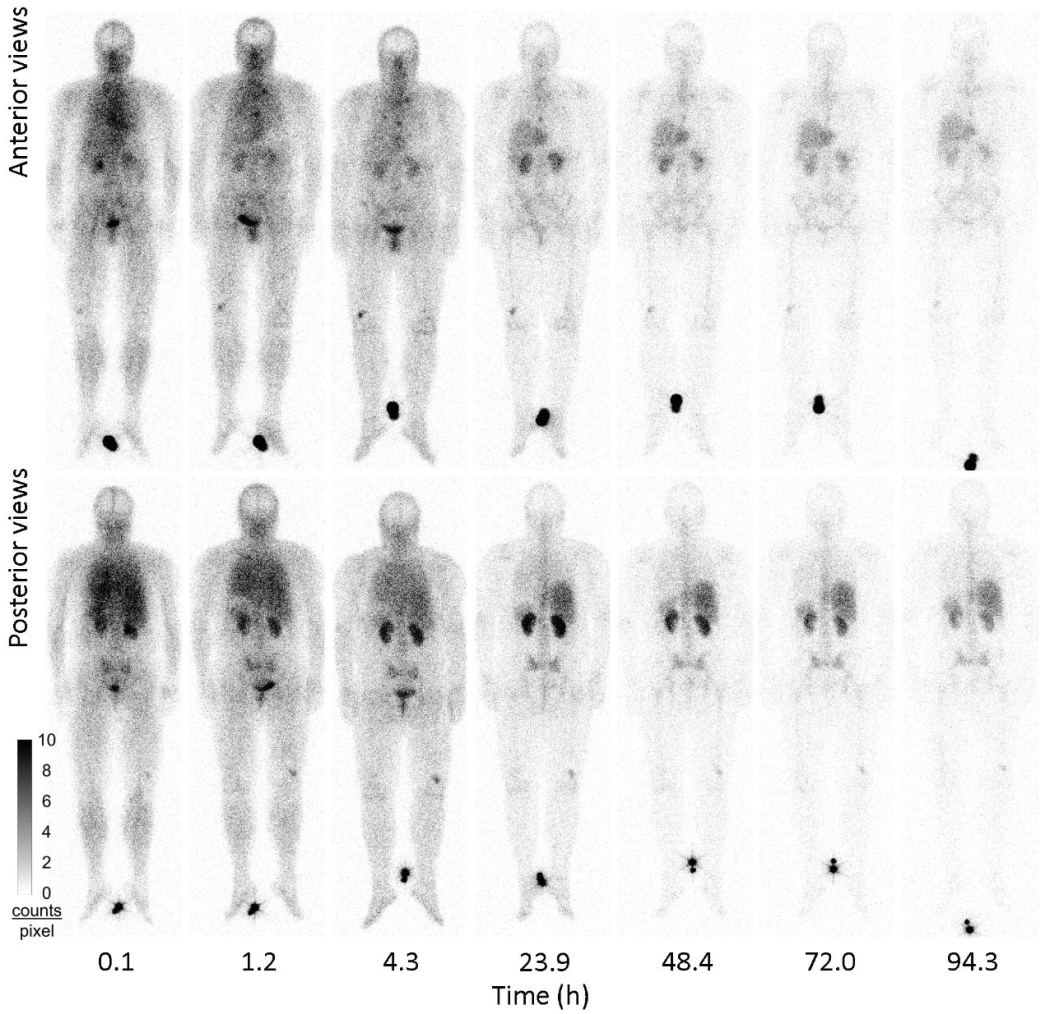

Supplemental Figure 1: Series of whole body scans of patient P3 after 197 MBq ^{177}Lu-Pentixather performed with the same gamma camera and identical camera settings, scan speed (10 cm/min), and measuring distance. The visible range of all images is 0 to 10 counts per pixel.

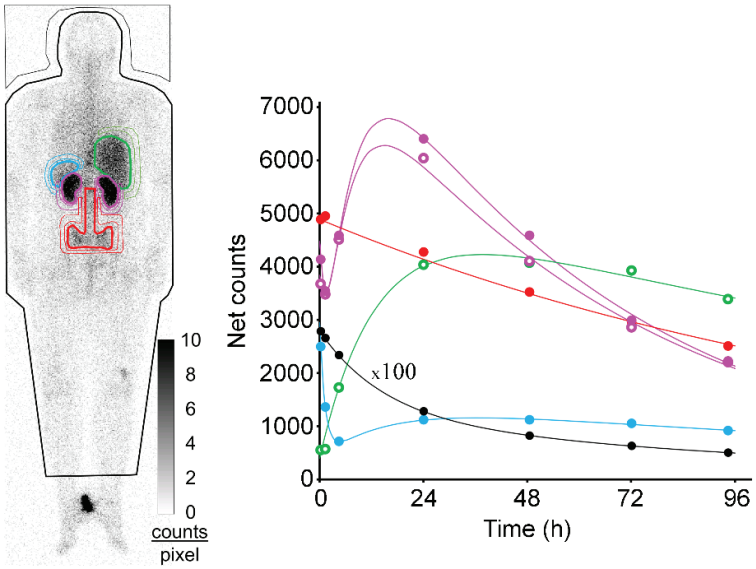

Supplemental Figure 2: Tissue and background ROIs in patient P3 and corresponding background-corrected net counts in the whole body (black dots), red bone marrow (red dots), liver (green circles), right (purple dots) and left (purple circles) kidneys, and spleen (blue dots) with respective fit functions. Whole body data were reduced by a factor of 100 for scaling.

Identical regions were copied to each scan in the series and background-corrected counts were extracted without further corrections e.g. for attenuation or scatter. While for kidneys, spleen, and red marrow net counts were derived from posterior images only, geometric mean of net counts in anterior and posterior views were calculated for the whole body and liver. The view used for lesions depended on the location and overlying accumulating structures. Given the long acquisition times, the net counts in the ROIs were found to be statistically sufficient to fit activity kinetics. For single kidneys, a median of 4980 net counts were registered in the scans after one day; 3 of 37 kidneys showed less than 2000 net counts (minimum: 932 in the right kidney of patient P15; Figure 1 in manuscript) and 3 more than 10000 net counts (maximum: 12248 in the right kidney of patient P19).

For most tissues, a bi-exponential decay function was fitted to the resulting net counts by ordinary least squares regression. Another short-lived exponential function was added when necessary to adequately reproduce the measured data up to 4 h (see spleen data in Supplemental Figure 2); the contribution to the integral under the curve, probably due to the perfusion effect, remained small in all cases. In the calculation of areas under the curves and from this time-integrated activity coefficients, the fit functions were assumed to be valid also for the time after the last measured value.

Tomographic imaging

The total body time-integrated activity coefficient was deduced by normalizing all net counts to those in the first scan at 0.1 h. For other tissues, kinetics were normalized to match the absolute activity uptakes measured one day (two days in patient P9) after the administration by SPECT/CT.

Tomographic images were acquired with a Siemens Symbia T2 or, in patients P1, P8, P12, P15, and P18 a Siemens Intevo Bold (Siemens Healthineers, Erlangen, Germany) over a rotation of 180° with 3° angular steps (= 2 x 60 frames) at 30 s per projection. For both dual head cameras used, data were acquired with medium energy collimators and a central 20% photopeak window at 208 keV between lower and upper 10% scatter windows. Data were reconstructed using an ordered subset expectation maximization algorithm with depth-dependent 3D resolution recovery (Siemens Flash-3D) with 6 subsets, 6 iterations, and a 6 mm Gauss filter for a 128x128 matrix with corrections for scatter and attenuation to obtain absolute activity quantification in voxels sized 0.11 cm^3.

For both cameras, the detection efficiency under the aforementioned imaging and reconstruction conditions was determined by measuring a large volume (6.9 L Jaszczak phantom) homogeneously filled with a known ^{177}Lu activity in a lutetium chloride carrier solution (10 µg inactive lutetium per g dissolved in 0.1 mol per L hydrochloric acid). Extensive measurements with phantoms of different volumes and shapes with and without scattering bodies and surrounding background activity indicated typical accuracies of 10% or less for volumes as large as human kidneys, where partial volume effects are of minor relevance.

Activity in accumulating tissues under consideration was typically entirely quantified in SPECT/CT by including all activity in a volume interest (VOI) defined by an isocontour that exceeded the tissue boundaries on CT by approximately 1 cm in all dimensions. Supplemental Figure 3 shows the boundaries of the VOIs in the pre-therapeutic SPECT/CT for the kidneys in patient P3.

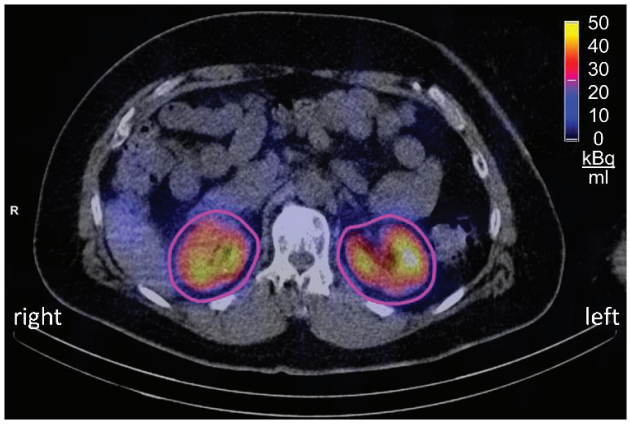

Supplemental Figure 3: Transverse plane of a SPECT/CT measured 24.7 h p.i. of 197 MBq ^{177}Lu-Pentixather in patient P3. SPECT image information was corrected for scatter and attenuation. Activity contents in the volumes of interest were 4.40 MBq for the left and 5.15 MBq ^{177}Lu for the right kidney.

Alternatively, in livers and enlarged spleens, where adjacent tissues with high activity concentration such as kidneys and tumorous lesions prevented the delineation of an isocontour VOI around the complete tissue, activity was quantified in a large subvolume within the organ and activity was scaled to the total mass measured by CT.

For the red bone marrow, the activity time function was determined in the planar images with a large ROI over pelvis and spine and normalized to the activity measured in SPECT/CT in L2-L4 in the lumbar spine, which was assumed to contain 6.7% of the total red marrow activity. In the absence of evidence of activity accumulation in bone, it was assumed that the measured activity was entirely located in bone marrow.

In order to estimate time-integrated activity coefficients, the activities measured by SPECT/CT were used for normalization of the kinetics deduced from the whole body scans. For example, activity in the right kidney of patient P3 was determined by SPECT/CT after 24.7 h to be 5.15 MBq ^{177}Lu corresponding to 2.23% of the administered activity. The fit function to the net counts of the right kidney in the planar whole-body scans (Supplemental Figure 2) indicated 6367 net counts after 24.7 h. The fit function to the net counts was normalized by a factor of 2.23% / 6367 to obtain the retention function shown in Figure 2 of the main manuscript, which was then integrated to calculate the time-integrated activity coefficient.

Uncertainties

The error to be assumed for the functions fitted to the whole body measurements depends on the kinetics and the uncertainty of the measured values. For the functions shown in Supplemental Figure 2, the fit yielded half-lives after ^{177}Lu-Pentixather of 47.5 h for the left kidney and 44.0 h for the right kidney. Assuming 5% relative error in single net count values and taking covariances into account, the statistical uncertainties are about 10% for the half-life values and about 5% for the areas under the curves. The uncertainties are about 15% and 7%, respectively, with 10% relative error in single net count values. Approximately one-third of the decays occur later than 72 h and one-fifth later than 96 h in a kidney with median kinetics parameters. Converted to ^{90}Y with its shorter physical half-life of 64 h, only about 17% of the decays occur later than 72 h and 9% later than 96 h.

The kinetics in tissues with long effective half-lives can be determined less accurately from measurements over four days. With 5% uncertainty in single net count values, the fit function shown in Supplemental Figure 2 for the liver corresponds to an effective half-live of 145 h ± 73 h for ^{177}Lu-Pentixather and 36% uncertainty of the area under the curve. Converted to the kinetics of ^{90}Y-Pentixather, the uncertainty of the area under the curve is reduced to 10%. The expected contribution from decays later than 96 h is 58% for ^{177}Lu and 23% for ^{90}Y in a liver with median kinetics parameters.

The error in activity measurement in tomography is derived from the calibration error, which is probably less than 10%, and statistical uncertainties in reconstruction and quantification. Measured ^{177}Lu activity concentrations in the right and left kidneys in our patients were in good agreement in most individuals. Only patients P17 and P18 with adrenocortical carcinoma showed large deviations with right to left activity concentration ratios of 1.36 and 0.70, respectively. In the other patients with two kidneys, this ratio was 1.03 ± 0.07, indicating typical statistical quantification errors in the order of 10%.

Post-therapeutic measurements

The first 4 patients P1 to P4 were treated with ^{177}Lu-Pentixather after pretherapeutic dosimetry (Supplemental Table 1). Except for P2 who received 23.5 GBq ^{177}Lu, these patients underwent a similar measurement program as in pretherapeutic dosimetry, but with shortened scan duration. The radiosynthesis for therapy followed the same protocol as for pretherapeutic dosimetry using higher amounts of Pentixather (200 µg) and gentisic acid (7 µg) per batch of 8 GBq $^{177}LuCl_3$.

Patient P3 received treatment with 7.8 GBq ^{177}Lu-Pentixather three weeks after pretherapeutic dosimetry, with whole body scans after 1, 4, 22, 48, 144, and 309 hours and SPECT/CT after 23 h. The posterior view acquired 1 day after the administration is shown in Supplemental Figure 4 together with the corresponding image from pre-therapeutic dosimetry. Data evaluation using the identical procedures as described above for pre-therapeutic dosimetry resulted in the retention values shown in Supplemental Figure 5.

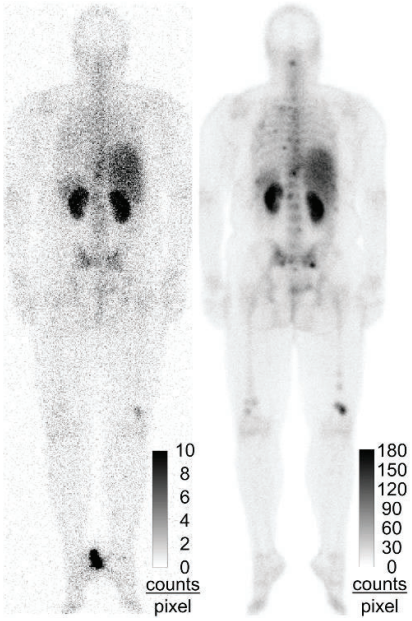

Supplemental Figure 4: Posterior whole body views of patient P3 24.1 h p.i. 197 MBq ^{177}Lu-Pentixather for pre-therapeutic dosimetry (left) and 22.2 h p.i. 7.8 GBq ^{177}Lu-Pentixather for therapy. Scanning speed was two times higher during therapy.

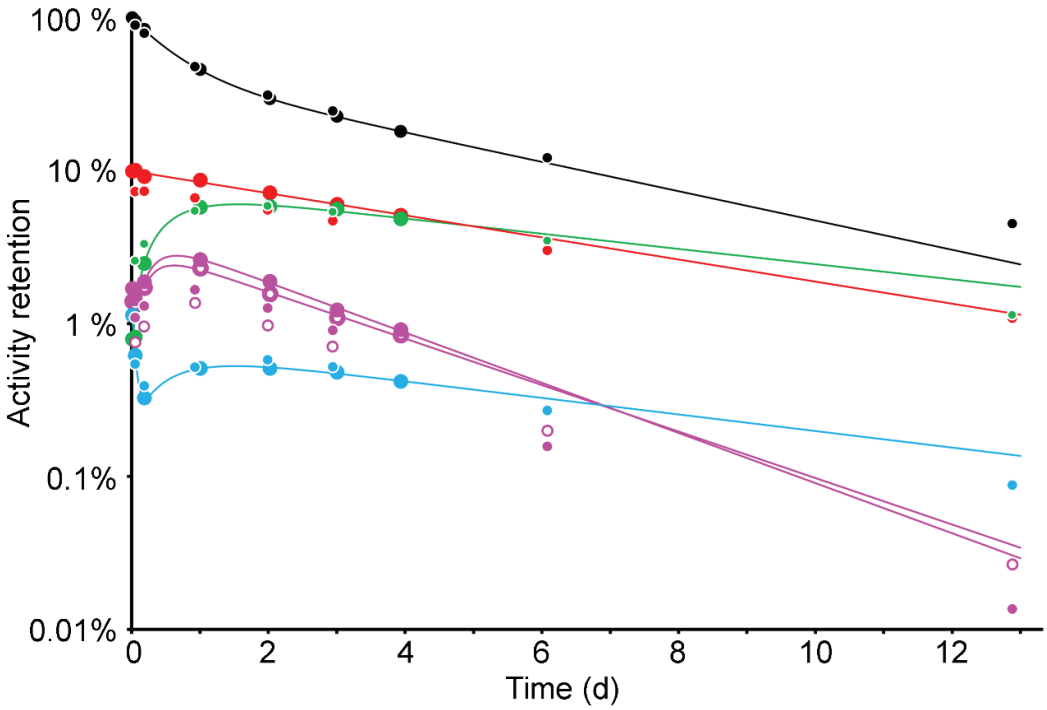

Supplemental Figure 5: Time functions of activity retention in the whole body (black dots), red bone marrow (red dots), liver (green dots), right (purple dots) and left (purple circles) kidneys, and spleen (blue dots) in patient P3. Large symbols indicate data measured after 197 MBq ^{177}Lu-Pentixather for pre-therapeutic dosimetry, small symbols data measured during therapy with 7.8 GBq ^{177}Lu-Pentixather. Solid lines show functions fitted to the dosimetry data and extrapolated to later times.

Retention values measured by SPECT/CT during therapy were 91 % of the corresponding pre-therapeutical values in liver, 99 % in spleen, 79 % in the spline, 60 % in left kidney, and 63 % in the right kidney. The shapes of the retention functions during therapy are generally well predicted by the dosimetric assessment, but the predictive power for late time points is limited, as expected.

Supplemental Table 3 lists the tissue absorbed doses per administered activity in patients P1, P3, and P4 with complete dosimetry after therapy with ^{177}Lu-Pentixather. Most time integrated activity coefficients are slightly reduced during therapy. Possible explanations are the higher injected activity and peptide mass during treatment and the altered clinical conditions such as an increased fluid intake and the infusion of amino acids. During dosimetry, no renal protective medication was administered because of the associated side effects.

The more pronounced reduction in retention in the kidneys suggests an effect of the amino acid infusion administered for renal protection. Since the effect of such a measure on a new radiopeptide cannot be easily estimated theoretically, the use of the medication was purely empirical with one of the most commonly used amino acid mixtures to competitively prevent reabsorption of the peptides in the renal tubules. To date, no attempts have been made to optimize the kidney protection medication for radiolabeled Pentixather.

Supplemental Table 3: Comparison of tissue absorbed doses per administered activity measured in pretherapeutic dosimetry and during therapy with ^{177}Lu-Pentixather in patients P1, P3, and P4. T/D indicates the averaged ratio of therapy to pretherapeutic dosimetry.

Patient	^{177}Lu-Activity	Kidneys (Gy/GBq)	Liver (Gy/GBq)	Spleen (Gy/GBq)	Red marrow (Gy/GBq)	Lesion (Gy/GBq)
P1	238 MBq	1.01	0.39	0.58	0.14	2.2
	15.2 GBq	0.59	0.38	0.49	0.11	2.5
P3	197 MBq	2.10	0.93	0.72	0.66	
	7.8 GBq	1.20	0.77	0.67	0.55	
P4	206 MBq	1.48	0.80	0.70	0.48	
	9.9 GBq	1.01	0.64	0.69	0.39	
T/D	51	61%	87%	92%	81%	114%